applied sciences

MDPI

Communication

Optical Radiation during Sputtering of Lithium into a Noble Gas Using a Nanosecond Electron Beam

Mendykhan Khasenov [1], Kuanysh Samarkhanov [1,2,*], Erlan Batyrbekov [3], Yuriy Gordienko [1], Inesh E. Kenzhina [4,5] and Yevgeniy Tulubayev [1]

[1] Institute of Atomic Energy Branch of National Nuclear Center of the Republic of Kazakhstan, Kurchatov 071100, Kazakhstan; mendykhan.khassenov@nu.edu.kz (M.K.); gordienko@nnc.kz (Y.G.); tulubaev@nnc.kz (Y.T.)
[2] Department of Physics and Technology, Sarsen Amanzholov East Kazakhstan University, Ust-Kamenogorsk 070000, Kazakhstan
[3] National Nuclear Center of the Republic of Kazakhstan, Kurchatov 071100, Kazakhstan; batyrbekov@nnc.kz
[4] Advanced Electronics Development Laboratory, Kazakh-British Technical University, 59 Tole bi St., Almaty 050000, Kazakhstan; kenzhina@physics.kz
[5] Department of General Physics, Satbayev University, Almaty 050013, Kazakhstan
* Correspondence: samarkhanov@nnc.kz

Abstract: The optical radiation in a gaseous medium upon the irradiation of a lithium layer with a fast electron beam of a 5 ns duration has been studied. The irradiation chamber was filled with argon, krypton, or xenon at a pressure of 10 kPa up to 60 kPa. The lines of lithium atoms appear in the emission spectrum at a lithium layer temperature of 650–680 K, and the intensity of these lines sharply increases with the increasing temperature of the lithium layer. The optical radiation arises from both the transitions of noble gas atoms and the transition of the lithium atom in a time of about 20–30 ns. The duration of the radiation pulses at half maximum at temperatures above 800 K was 60–100 ns at a wavelength of 610.4 nm and 140–220 ns at 670.8 nm in krypton and argon. The various mechanisms for the population of lithium levels during the radiation pulse are discussed.

Keywords: sputtering; lithium; noble gases; electron accelerator; luminescence

check for updates

Citation: Khasenov, M.; Samarkhanov, K.; Batyrbekov, E.; Gordienko, Y.; Kenzhina, I.E.; Tulubayev, Y. Optical Radiation during Sputtering of Lithium into a Noble Gas Using a Nanosecond Electron Beam. *Appl. Sci.* **2023**, *13*, 3669. https://doi.org/10.3390/app13063669

Academic Editor: Roberto Sacchi

Received: 31 January 2023
Revised: 3 March 2023
Accepted: 10 March 2023
Published: 13 March 2023

Copyright: © 2023 by the authors. Licensee MDPI, Basel, Switzerland. This article is an open access article distributed under the terms and conditions of the Creative Commons Attribution (CC BY) license (https://creativecommons.org/licenses/by/4.0/).

1. Introduction

Interest in the sputtering of lithium into a gaseous medium using charged particles is associated with the possibility of excitation of large volumes of gas caused by $^{6}Li(n,\alpha)^{3}H$ nuclear reaction products [1]. The processes during the sputtering of metals caused by nuclear particles in a gaseous medium [1,2] are significantly different from the processes of sputtering into vacuum caused by accelerated ions [3]. Cadmium and zinc sputtering into helium upon irradiation by nuclear particles was investigated in [2,4]. At temperatures above 430 K, an exponential increase in the intensity of the cadmium ion lines was observed. The temperature dependence of the luminescence intensity is explained [2] using the droplet model of atomic nuclei. A nuclear particle dislodges some of the atoms from a crystal lattice into internodes; some of the displaced atoms may be in the excited state during braking in the metal. The rapid heating and release of heated metal micro-droplets occur due to the particle kinetic energy. The displaced atoms diffuse inside the droplet in the vacancies search. The self-diffusion coefficient sharply increases, which contributes to the displaced atom output from the droplet at the cadmium temperature of 430–530 K.

It should be noted that the metal temperature in the drop will be about or above the melting point and is loosely related to the initial temperature. Accordingly, the self-diffusion of displaced atoms from the base metal should be considered.

In [5], mass-spectrometric studies of sputtering caused by fast heavy ions of metals, semiconductors, and ionic crystals were carried out. The sputtering of materials under in

situ irradiation ions with an energy of 4.8 MeV/u of ^{197}Au and ^{48}Ca was investigated using time-of-flight mass spectrometry in combination with laser post-ionization. In previous studies [6], catcher foils were used to collect the ejected material. It has been shown that most of the material sputtered from a solid surface under irradiation with fast heavy ions are emitted in a neutral state. In [5], a mass-resolved comparison of secondary ions and neutral particles was created for the first time for separately determining the composition of the sputtered flux and the ion fractions of different emitted species. In most cases, most of the sputtered material is emitted in the neutral state, with the flux of sputtered particles mainly consisting of single atoms and small (mostly diatomic) clusters [5].

In [1,7], a different mechanism from [2] was proposed for the appearance of lithium lines upon the irradiation of a lithium layer in a gaseous medium by products of the ^{6}Li(n,α)^{3}H nuclear reaction.

From the analysis of the dependence of the intensity of noble gas and lithium atoms lines on the temperature of the lithium layer, it is concluded that the main channel leading to the population of the lithium levels is the Penning process with noble gas atoms (R) in the 1s-state:

$$R^*(1s) + Li \rightarrow Li^+ + R + e \quad (1)$$

Further plasma–chemical-reaction molecular ions of Li_2^+ are formed. During the process of the dissociative recombination of ion:

$$Li_2^+ + e + R \rightarrow Li + Li^* + R, \quad (2)$$

excited lithium atoms are formed.

The rapid increase in the luminescence intensity is well approximated by [1]:

$$I \sim \exp\left(-\frac{A}{kT}\right) \quad (3)$$

where A is the activation energy of this process. The A values obtained for 610.4 nm lithium lines are 1.67 eV in argon, 1.63 eV in neon, and 1.61 eV in xenon. These values are in good agreement with the evaporation energy of lithium, which is equal to 1.63 eV (156.9 kJ/mol [8]). It can be assumed that the sputtering of lithium is due to the evaporation in the nuclear particle channel [1]. For the ion energies in the MeV range, the electronic sputtering processes contribute to the surface sputtering [6,9]. A major part of the energy of the heavy ions is transferred to electrons along the ion track. A coupling between the electrons and phonons causes large local heating in the cylindrical volume. The surface atoms may be removed through evaporation in a jet from the heated volume [6].

The selective deactivation of the 1s-levels of noble gases indicates the possibility of creating a laser at 2p-1s transitions of noble gas atoms with the deactivation of the lower laser level caused by lithium atoms when excited by the products of the ^{6}Li(n,α)^{3}H nuclear reaction or electron beam [10,11]. In such a laser device, the gas medium is excited by the products of a nuclear reaction and the sputtered lithium deactivates the lower 1s laser level in processes (1). From the point of view of creating a laser with 2p-1s transitions of noble gases, excited by an electron beam, it is of interest to study the sputtering of lithium into gas using a pulsed electron beam bombardment. The sputtering of lithium caused by electrons with energies of hundreds of keV may be different from the sputtering caused by MeV ions.

In [1,7,11], studies were carried out on a stationary nuclear reactor under continuous irradiation of the gaseous medium and the lithium layer. The studies with short, nanosecond pulse pumping alongside the preliminary studies that were carried out on a stationary nuclear reactor, may be useful to clarify the excitation mechanisms of the lithium atoms and gaseous medium and the lithium sputtering processes. The spectral–temporal characteristics of luminescence upon the irradiation of a lithium layer in a noble gas medium with a nanosecond electron beam were measured to investigate the mechanisms of the population of lithium levels.

2. Materials and Methods

The research was carried out on the experimental setup, as shown in Figure 1.

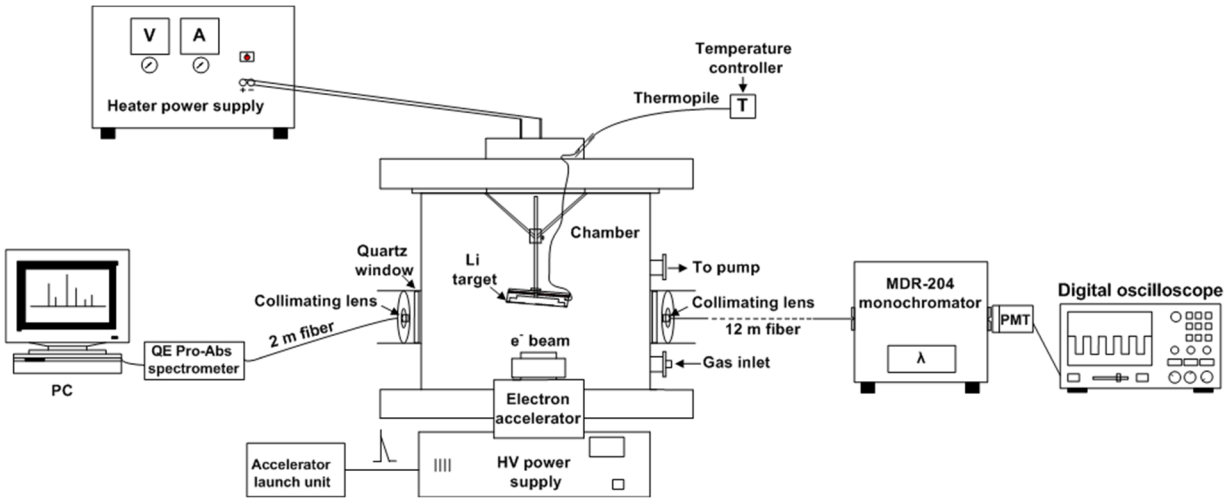


Figure 1. Scheme of the experimental setup.

An X-ray tube with an explosive cathode generates an electron beam, with an energy of about 150 keV and a duration of 5 ns [12]. The electrons were led into the gas through a 150 μm thick beryllium window. The calculations were performed using the Casino software to estimate the energy of the electrons at the output from the beryllium window. The Casino software uses the Monte Carlo method to simulate the interaction of a beam of electrons and matter and can be used to calculate the interaction of the low-energy electrons with the solids [13]. This program is widely used in studies of cathodoluminescence [14,15] and lasers with electron beam pumping [16]. It has been shown in [17] that Casino is quite precise (maximum error 10%) to simulate an electron pathway with energy of about 10 keV.

The following conditions were chosen for the simulation:

- Mono-energy electrons with an energy of 150 keV were used;
- The minimum energy of the initial electrons monitored using the software was 0.05 keV;
- The possibility of secondary electron formation through the collisions of the initial electrons in the beryllium window was considered.

The simulations using the Casino software showed that the electron energy at the output from the beryllium window ranges from 0 to 105 keV, with an average electron energy of 49 keV.

To simulate the processes during the excitation of the noble gas atom and lithium caused by the $^{6}Li(n,\alpha)^{3}H$ nuclear reaction products, a special target node was developed. The target node consisted of a metal cuvette, on which an ohmic heater, a 30 mm diameter lithium capillary porous structure (CPS), a movable rod enabling adjustment of the distance of the lithium target from the cathode, an ohmic heater, connected to a ceramic-insulated hermetic connector, a Cr-Al-type thermocouple, and leads for thermocouples and current leads were attached. A DC power supply (B5-21) was used in the manufacturing process of the lithium CPS, which produced a continuously adjustable DC stabilized voltage and a current. As a CPS, a matrix of 12Cr18Ni10Ti stainless steel was used, which was a woven mesh with a cell size of about 100 μm and a thickness of 0.1 mm. CPS was used to ensure the stabilization of the lithium in the liquid state during the experiments above the melting point of lithium. The lithium target was mounted on the top of the viewport with a slight angle of inclination. The tilt angle of the lithium target did not exceed 5°. The temperature of the lithium target was measured using a thermocouple and the gas temperature was not controlled.

Lithium CPS was directly fabricated in the experimental chamber of the experimental setup. For these purposes, a cuvette with a diameter of 30 mm was created. A 12Cr18Ni10Ti stainless steel cuvette was clamped with a washer for a snug fit with the rod. Before the preparation of the lithium target, the CPS matrix was placed in a solution of concentrated nitric (HNO_3) acid and washed in alcohol in stages, using a ProsKit SS-803F ultrasonic cleaner.

The methods, techniques, and procedures for purifying lithium metal used in this work are described in detail in the monograph *Lithium* [18]. The CPS matrix filling procedure using lithium was carried out using previously developed and experimentally tested techniques [19].

The procedure of loading lithium into the cuvette was carried out in an argon box to minimize the interaction of lithium with impurities (N_2, CO_2, O_2, H_2, etc.). Further, the stainless-steel mesh was spot welded into the cuvette with the loaded lithium. To achieve a more uniform heating of the test sample and minimize the temperature gradients over the volume of the lithium CPS, an ohmic heater was wound around the outer circumference of the target. A hole for a CrAl-type thermocouple was drilled on the inner side of the cuvette. The temperature changes were recorded using a DTB 9696 temperature controller. A hermetically sealed connector was installed on the lid of the experimental chamber for switching the thermocouple and the ohmic heater. The next step was to install the target node with the lithium CPS into the experimental chamber of the setup, which was pre-filled with argon. The next step was to fill the matrix of the metal CPS with lithium.

In general, the procedure for the manufacture of lithium CPS was as follows:

- Heat the lithium using the ohmic heater to a temperature of about 523 K and condition it at this temperature for 1 h under continuous vacuum pumping using a fore-vacuum pump;
- Supply the argon into the chamber up to a pressure of about 30 kPa;
- Heat the lithium target to a temperature of 773 K and condition it at this temperature for ~45 min;
- Heat the lithium target to a temperature of 900 K and condition it at this temperature for ~30 min;
- Let the temperature decrease to 573 K and condition it at this temperature for ~15 min;
- Turn off the heating and pump the argon out from the installation chamber at a temperature of 453 K.

During the visual observation from the quartz window, according to the outer view and typical metallic luster typically for lithium, it was found that the porous material was completely filled with lithium. A visual illustration, showing the complete filling of the metal mesh with lithium is shown in Figure 2 below.

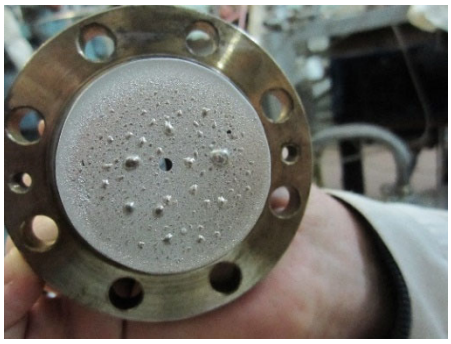


Figure 2. Appearance of lithium target after the irradiation with an electron beam.

The chamber was covered with a white layer by the end of the measurements, including the quartz windows and the beryllium window. The layer was relatively easy to clean off, the dusting of the window had no noticeable effect on the light transmission.

It is pointed out here that picture in Figure 2 was taken after the end of the irradiation of a lithium layer with an electron beam. The trace of the electron beam can be seen, as

outgrowths, formed as a result of the lithium target heating to high temperatures during the measurements.

The use of the above-described method of manufacturing a lithium target allowed for obtaining a lithium CPS with the required technical characteristics.

The distance from the beryllium cathode window to the target was 30 mm. The irradiation chamber was filled with argon, krypton, or xenon at a pressure up to 60 kPa.

The optical radiation was led out of the chamber through two quartz windows; light from the first window led through a 2m long fiber-optic cable to the QEPro-Abs spectrometer (Ocean Insight, Singapore). The emission spectrum was recorded in 15 s, with 20 pulses of the electron beam passed through during this time. The light from the second window was led through a 12 m long fiber-optic cable to another room to record the temporal parameters of the optical radiation, using the PDM02-9113-CN (ET Enterprises, Uxbridge, UK) photomultiplier module (PMT) and the MDR-204 monochromator. The photomultiplier was operated in current mode with a 50-Ohm load and the temporal signal was recorded on the screen of the Tektronix TBS2204B digital oscilloscope. The line intensities were measured using an optical spectrometer or PMT and are provided without correction for the spectral sensitivity of the setup.

3. Results

The lines of the 2p-1s atomic transitions (Paschen notation) predominate in the emission spectra of the noble gases at temperatures of ≈300 K. At a lithium layer temperature of 650–680 K, the lithium lines appear in the emission spectrum (Figure 3); the brightest are 812.6 nm (3s-2p), 610.4 nm (3d-2p), and the resonant lines at 670.8 nm (2p-2s). All the wavelengths are rounded without dividing them into separate multiplets. In contrast to [1,7], there are no sodium and potassium lines in the emission spectrum, because high purity (99.9%) lithium was used. The lithium lines appeared at a lower temperature (520–600 K [1,7]) upon excitation caused by nuclear reaction products with energies up to 2.7 MeV.

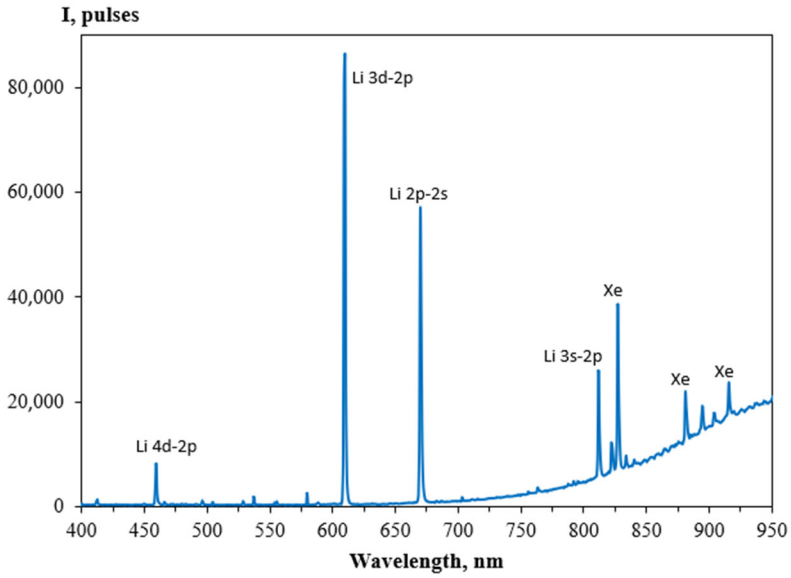


Figure 3. Emission spectrum at a pressure of xenon 10 kPa and temperature of the lithium layer 870 K. The continuous spectrum in the IR region is associated with the thermal radiation of the lithium layer.

The intensity of the lithium lines sharply increases with the increasing temperature and can be several times higher than the intensity of the lines of the noble gas atoms (Figure 4). The emission in the resonance lines of the lithium at 670.8 nm was "trapped" and prone to self-absorption. The radiation trapping consists of multiple re-emissions and reabsorptions of resonance photons in an optically dense medium. In the resulting photon

flux, extending beyond the system, the most numerous (and the most strongly absorbed) photons from the center of the line do not predominate but relatively few photons from distant line wings do, as they have a free path that is comparable to the size of the system. The radiation at 610.4 nm is also trapped in argon.

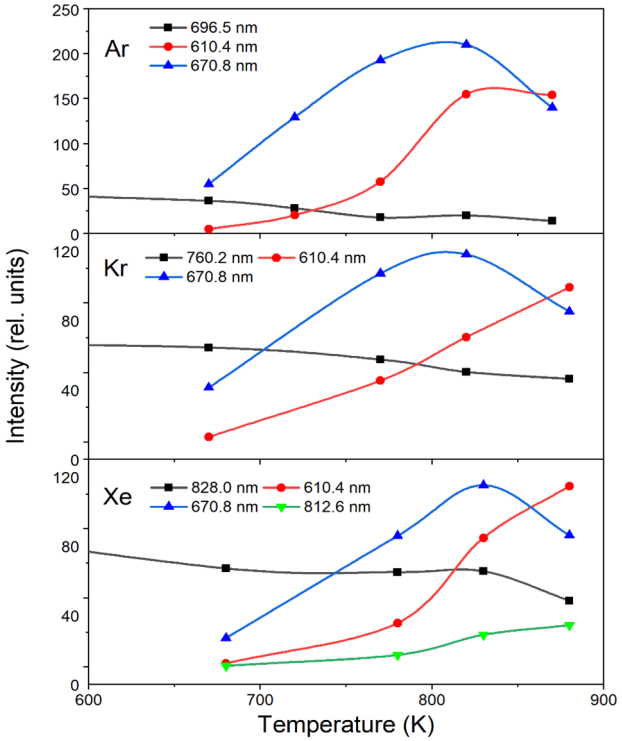


Figure 4. Dependence of the intensity of the lines of atoms of lithium and noble gases in argon, krypton, and xenon on the lithium layer temperature. The initial gas pressure at 295 K: Ar—40, Kr—30, and Xe—10 kPa.

Figure 5 shows the dependence of the emission intensity of the krypton and lithium atom lines on the krypton pressure. The intensity of the krypton line at 760.2 nm (transition $2p_6$-$1s_5$) increases up to a pressure of 20 kPa then reaches a plateau. The increase in the energy nested to the gas is balanced for by the quenching of the $2p_6$ level by the krypton atoms. The intensity of the lithium resonance line decreases by 2 times but does not drop to 0 when the krypton pressure is increased from 20 to 60 kPa. The electron path with an energy of 50 and 100 keV in krypton at a pressure of 60 kPa are 33 mm and 107 mm, respectively [20].

The intensities of the lines of the p–s transitions of noble gases monotonically decrease with the increasing temperature or practically do not change. There is no kink in the curves of the dependence of line intensity of the 2p-1s transitions of the noble gas atoms on the temperature with a sharp increase in the intensity of the lithium lines. From similar dependencies in [1,7], we can conclude that the main channel leading to populating the 2p-levels of the lithium seems to be process (1) involving the 1s levels of the noble gas atoms.

Figure 6 shows oscillograms of the radiation at the transitions of the lithium and noble gas atoms.

The oscilloscope was triggered by the noise of the positive polarity upon the breakdown of the spark gap sharpener. The duration of the radiation pulses at half maximum at temperatures above 800 K was 60–100 ns at a wavelength of 610.4 nm and 140–220 ns at 670.8 nm in krypton (Figure 5) and argon. Figure 6c shows the shape of the radiation pulses in xenon at a lithium layer temperature of 770 K, when there is still no self-absorption on the lithium resonance line. The pulse duration of the emission of the resonance line of lithium at 670.8 nm (330 ns) was significantly higher than the duration of emission of xenon

at 828.0 nm (70 ns). This seems to be due to the transfer of excitation from the metastable levels of the xenon atom.

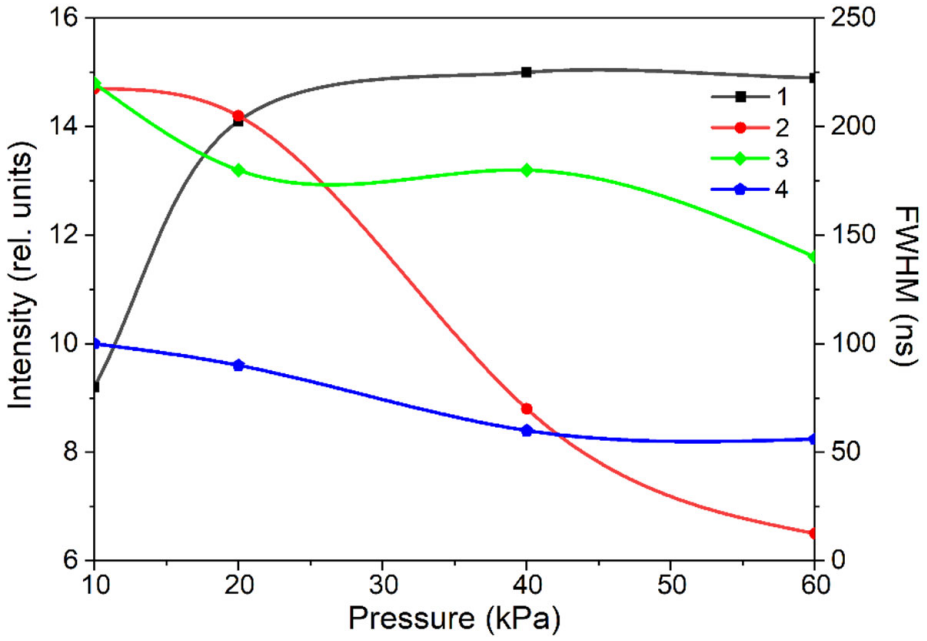
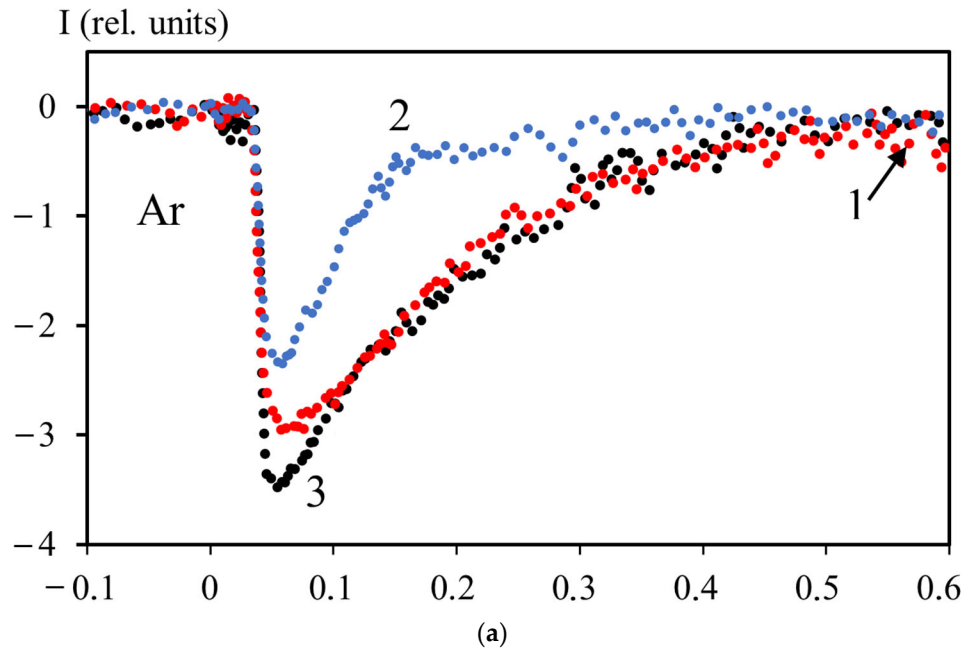


Figure 5. Dependence of the intensity of the lines of krypton (1, in black, 760.2 nm) and lithium (2, in red, 670.8 nm) on krypton pressure. Dependence of the emission duration (FWHM) on the 670.8 nm (3, in green) and 610.4 nm (4, in blue) lithium lines on the krypton pressure. Lithium layer temperature 870 K.



(**a**)

Figure 6. *Cont.*

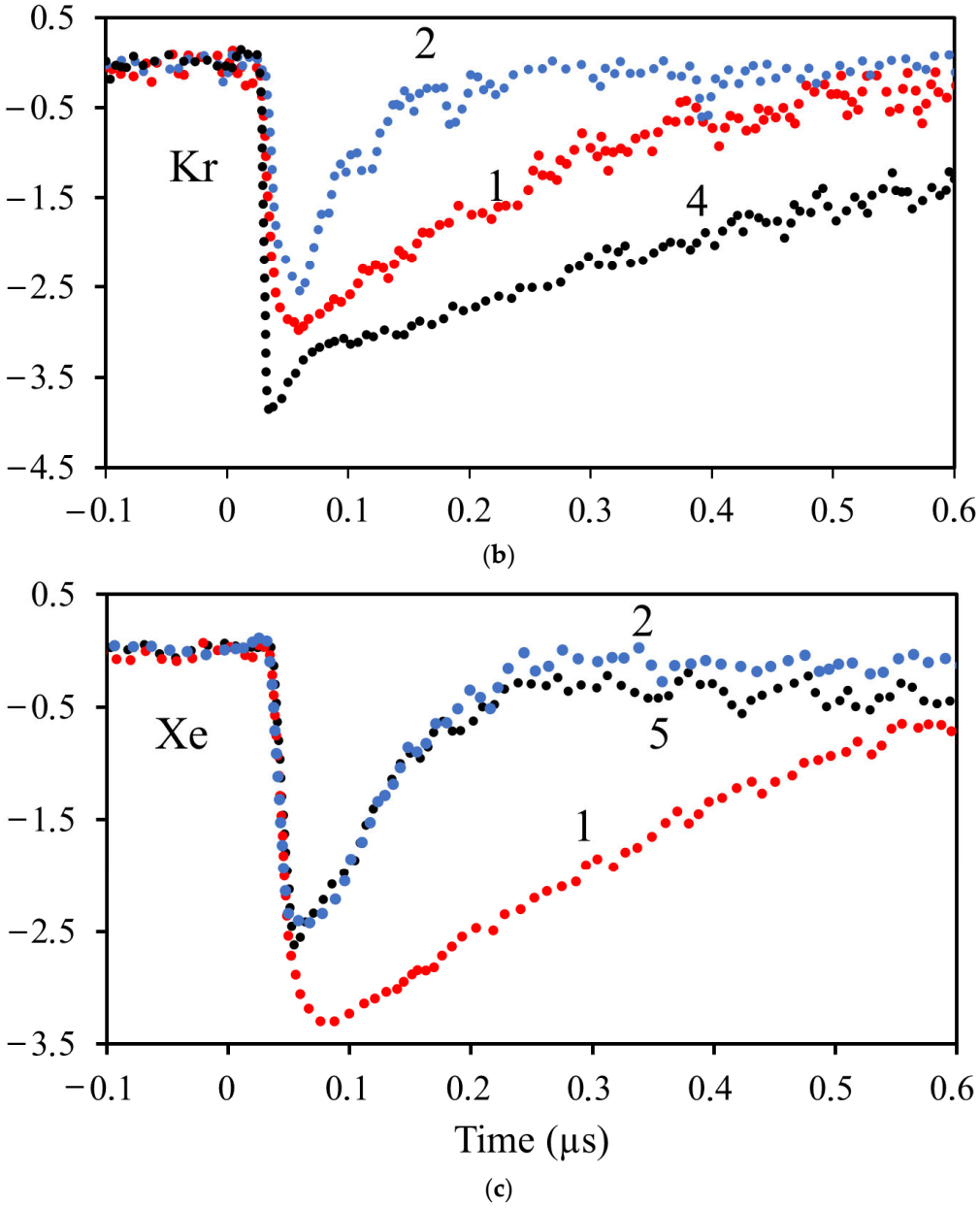


Figure 6. Oscillograms of radiation on lines of lithium 670.8 nm (1, in red), 610.4 nm (2, in blue), argon 696.5 nm (3, in black scatter, in Figure 6a), krypton 760.2 nm (4, in black scatter, in Figure 6b), and xenon 828.0 nm (5, in black scatter, in Figure 6c). The initial pressure at 295 K of argon and krypton is 40 kPa, xenon 10 kPa, and lithium layer temperature 870 K (**a**), 820 K (**b**), and 770 K (**c**).

4. Discussion

As can be seen from Figure 4, with an increase in the lithium layer temperature from 670 to 870 K, the lithium line intensity increases from 3 to 4 times, while the saturation vapor pressure of the lithium at these temperatures increases by ≈500 times. The radiation on the lines of the lithium atom cannot be explained by the thermal evaporation of the lithium. Consequently, the lithium vapor density, which is different from the density of the saturated steam, is generated in the gas excitation area.

The sputtering mechanism here seems to have been somewhat different, unrelated to the displacement of the crystal lattice atoms and analogous to the electron sputtering caused by the MeV-ions. A major part of the energy of the heavy ions is transferred to the electrons along the ion track. A coupling between the electrons and phonons causes

large local heating in cylindrical volume. The surface atoms may be removed through evaporation in a jet from the heated volume [6].

The lithium at temperatures 1.5–2 times the melting point (453 K) was in a liquid state. This facilitates lithium evaporation in the fast electron track. As far as we know, there is no developed theory of sputtering from liquid metal.

The optical radiation arises from both at the 2p-1s transitions of the noble gas atoms and the transitions of the lithium atom in a time of about 20–30 ns (see Figure 6). The characteristic time of the plasma–chemical reactions in a gas is hundreds of nanoseconds; the luminescence of the lithium during the initial period cannot be explained by the processes in the plasma.

In [1], upon the irradiation of a lithium layer at a residual gas pressure of 10 Pa with the products of the $^{6}Li(n,\alpha)^{3}H$ nuclear reaction, the radiation intensity of the lithium lines was at least 10^4 times lower than during irradiation in a gaseous medium. The emission of the excited atoms during lithium sputtering by the products of the nuclear reaction does not contribute much to the emission of the lithium atoms, as compared with the plasma–chemical processes in the noble gas medium using sputtered lithium.

Apparently, in the case of bombardment caused by fast electrons, the radiation in the lithium lines during the initial period cannot also be explained by the sputtering of the excited lithium atoms under the influence of an electronic beam.

The similarity of the time dependence of the intensities of the noble gas and lithium lines suggests that the optical radiation from the noble gas atoms and lithium atoms during this period is formed by the same processes. The radiation on the lines of the 2p-1s transition of the noble gas atoms in the initial period is associated with the excitation of atoms caused by secondary electrons [21]. The excitation of the levels of noble gas atoms arises in the processes with electrons, with energies above the electron excitation threshold (Im); the Im for argon is 11.55 eV and for xenon is 8.315 eV. When xenon is irradiated with argon ions at 70 MeV, about 12% of the radiation is due to direct excitation caused by secondary electrons [22]. Most of the optical radiation from the noble gases is due to the dissociative recombination of the molecular ions (R_2^+, R_3^+) with the electrons in the plasma [23,24].

In the sub-threshold region (energy of the electrons is less than Im), the electrons lose their energy in elastic collisions with noble gas atoms, as well as during the excitation of the lithium atom levels. The thermalization time of the electrons in noble gases is 5–10 ns [21].

Thus, it can be assumed that the rapid increase in the radiation intensity of lithium atoms at the initial moment is due to the excitation caused by the secondary electrons in the sub-threshold region. The collisions of the excited atoms and ions with the lithium layer led to the release of free electrons from the surface, since the excitation energies of the atoms and ions are higher than the work function for lithium [25]. The quenching of the excited atoms and noble gas ions on the surface of the lithium layer, in this case, does not lead to the formation of excited lithium atoms.

Subsequently, the optical radiation is formed by the plasma–chemical reactions in the gas volume; the main reactions are provided in [1]. At lithium layer temperatures, when the saturated vapor pressure of lithium is low (10^{-6}–10^{-1} Pa) [1,7]), the required lithium vapor density ($\geq$1 Pa, [7]) is provided by the sputtering of the lithium caused by nuclear particles. During this experiment, the radiation of the lithium layer was observed at temperatures of 670–870 K, with the pressure of the saturated lithium vapor being 10^{-2}–7 Pa [26,27]. The source of the lithium at temperatures above 800 K is both thermal evaporation and lithium sputtering under the influence of an electron beam.

5. Conclusions

The spectral–temporal characteristics of optical radiation upon the irradiation of a lithium layer with a pulsed nanosecond beam of fast electrons in an argon, krypton, and xenon medium were investigated. The lines of lithium atoms appear in the emission spectrum at a lithium layer temperature of 650–680 K, and the intensity of these lines sharply increases with the increasing temperature of the lithium layer. The similar time

dependence of the intensities of the noble gas and lithium lines suggests that the optical radiation from the noble gas atoms and lithium atoms during this period is formed by the same processes. The optical radiation on the transitions of lithium atoms at the outset arises from the excitation of atoms caused by secondary electrons. Subsequently, the optical radiation is formed during the plasma–chemical reactions in the gas volume with the participation of the lithium atoms, obtained by both the thermal evaporation and sputtering under the influence of an electron beam.

Author Contributions: Conceptualization, M.K.; methodology, Y.G.; formal analysis, M.K.; investigation, K.S.; resources, Y.G.; data curation, K.S. and Y.T.; writing—original draft preparation, M.K.; writing—review and editing, I.E.K. and K.S.; visualization, K.S.; supervision, E.B.; project administration, E.B.; funding acquisition, E.B. All authors have read and agreed to the published version of the manuscript.

Funding: This research was funded by the Ministry of Energy of the Republic of Kazakhstan within the framework of the scientific and technical program "Development of nuclear energy in the Republic of Kazakhstan for 2021–2023 years" (IRN-BR09158470).

Institutional Review Board Statement: Not applicable.

Informed Consent Statement: Not applicable.

Data Availability Statement: Not applicable.

Acknowledgments: The authors express their gratitude to specialists of the Material Testing Department of the Institute of Atomic Energy, branch of the National Nuclear Center of the Republic of Kazakhstan for professional assistance and advice in obtaining the results.

Conflicts of Interest: The authors declare no conflict of interest.

References

1. Batyrbekov, E.; Khasenov, M.; Gordienko, Y.; Samarkhanov, K.; Ponkratov, Y. Optical radiation from the sputtered species under gas excitation by the products of the ^{6}Li(n,α)^{3}H nuclear reaction. *J. Lumin.* **2020**, *220*, 116973. [CrossRef]
2. Miskevich, A.I. Lasing on the $5s_2\ ^2D_{5/2}$ Cd II ion transition upon sputtering of metal cadmium by nuclear particles. *Quantum Electron.* **2002**, *32*, 803–810. [CrossRef]
3. Jensen, K.; Veje, E. An Experimental Study of Optical Radiation from Sputtered Species. *Z. Phys.* **1974**, *269*, 293–300. [CrossRef]
4. Mis'kevich, A.I.; Tao, L. Temperature Characteristics of Luminescence of ^{3}He–Zn High-Pressure Plasma under Nuclear Pumping. *Opt. Spectr.* **2008**, *105*, 691–698. [CrossRef]
5. Breuer, L.; Ernst, P.; Herder, M.; Meinerzhagen, F.; Bender, M.; Severin, D.; Wucher, A. Mass spectrometric investigation of material sputtered under swift heavy ion bombardment. *Nucl. Inst. Methods Phys. Res. B* **2018**, *435*, 101–110. [CrossRef]
6. Assmann, W.; Toulemonde, M.; Trautmann, C. *Sputtering by Particle Bombardment, Experiments and Computer Calculations from Threshold to MeV Energies*; Electronic Sputtering with Swift Heavy Ions; Behrisch, R., Eckstein, W., Eds.; Springer-Verlag: Berlin/Heidelberg, Germany, 2007; pp. 401–450. [CrossRef]
7. Gordienko, Y.; Khasenov, M.; Batyrbekov, E.; Samarkhanov, K.; Ponkratov, Y.; Amrenov, A. Emission of noble gases and their mixtures with lithium excited by products of ^{6}Li(n,α)^{3}H nuclear reaction. *Laser Part. Beams* **2019**, *37*, 18–24. [CrossRef]
8. Henriquesa, D.; Motalova, V.; Benczea, L.; Markus, T. Experimental Thermodynamics of New Electrode Materials for Li-Ion Batteries. *ECS Trans.* **2013**, *46*, 303–312. [CrossRef]
9. Behrisch, R.; Eckstein, W. *Sputtering by Particle Bombardment: Experiments and Computer Calculations from Threshold to MeV Energies*; Introduction and Overview; Springer-Verlag: Berlin/Heidelberg, Germany, 2007; pp. 1–20. [CrossRef]
10. Batyrbekov, E.; Khasenov, M.; Gordienko, Y.; Samarkhanov, K.; Kenzhina, I.E.; Kotlyar, A.; Miller, A.; Tskhe, V.; Bochkov, V. Experimental Facility to Study the Threshold Characteristics of Laser Action at the p-s-Transition of Noble Gas Atom upon Excitation by 6Li(n,α)3H Nuclear Reaction Products. *Appl. Sci.* **2022**, *12*, 2889. [CrossRef]
11. Samarkhanov, K.; Khasenov, M.; Batyrbekov, E.; Kenzhina, I.; Sapatayev, Y.; Bochkov, V. Emission of Noble Gases Binary Mixtures under Excitation by the Products of the ^{6}Li(n,α)^{3}H Nuclear Reaction. *Sci. Technol. Nucl.* **2020**, *2020*, 8891891. [CrossRef]
12. Gordienko, Y.N.; Khasenov, M.U.; Batyrbekov, E.G.; Amrenov, A.K.; Samarkhanov, K.K.; Ponkratov, Y.V. Luminescence of Noble Gases and Their Mixtures Under Nanosecond Electron-Beam Excitation. *J. Appl. Spectrosc.* **2018**, *85*, 600–604. [CrossRef]
13. Hovington, P.; Drouin, D.; Gauvin, R.; Joy, D.C.; Evans, N.D. CASINO: A new monte Carlo code in C language for electron beam interactions—Part III: Stopping power at low energies. *Scanning* **1997**, *19*, 29–35. [CrossRef]
14. Toth, M.; Phillips, M.R. Monte Carlo modeling of cathodoluminescence generation using electron energy loss curves. *Scanning* **1998**, *20*, 425–432. [CrossRef]

15. Drouin, D. CASINO a Powerful Simulation Tool for Cathodoluminescence Applications. *Microsc. Microanal.* **2006**, *12* (Suppl. 2), 1512–1513. [CrossRef]
16. Skrobol, C.; Heindl, T.; Krücken, R.; Morozov, A.; Steinhübl, R.; Wieser, J.; Ulrich, A. A miniature electron beam pumped laser. *Eur. Phys. J. D* **2009**, *54*, 103–109. [CrossRef]
17. Morozov, A.; Heindl, T.; Skrobol, C.; Wieser, J.; Krücken, R.; Ulrich, A. Transmission of ∼10 keV electron beams through thin ceramic foils: Measurements and Monte Carlo simulations of electron energy distribution functions. *Eur. Phys. J. D* **2008**, *48*, 383–388. [CrossRef]
18. Subbotin, V.I.; Arnoldov, M.N.; Ivanovsky, M.N.; Mosin, A.A.; Tarbov, A.A. *Lithium*; IzdAT: Moscow, Russia, 1999; 262p. Available online: https://www.rfbr.ru/rffi/ru/books/o_66904#1 (accessed on 11 March 2023)ISBN 5-86656-088-7.
19. Batyrbekov, E.G.; Gordienko, Y.N.; Ponkratov, Y.V.; Khasenov, M.U.; Tazhibayeva, I.L.; Barsukov, N.I.; Kulsartov, T.V.; Zaurbekova, Z.A.; Tulubayev, Y.Y.; Skakov, M.K. Development of the reactor lithium ampoule device for research of spectral-luminescent characteristics of nuclear-excited plasma. *Fusion Eng. Des.* **2017**, *117*, 204–207. [CrossRef]
20. The ESTAR Program. Available online: https://physics.nist.gov/PhysRefData/Star/Text/ESTAR.html (accessed on 30 January 2023).
21. Mel'nikov, S.P.; Sinyanskii, A.A.; Sizov, A.N.; Miley, G.H. *Lasers with Nuclear Pumping*; Springer: New York, NY, USA, 2015; p. 455.
22. Khasenov, M. Emission and level population in noble gases and their binary mixtures under ion beam excitation. *Nucl. Instrum. Methods Phys. Res. B* **2020**, *482*, 45–52. [CrossRef]
23. Ivanov, V.A. Dissociative recombination of molecular ions in noble-gas plasmas. *Sov. Phys. Uspekhi* **1992**, *35*, 17–36. [CrossRef]
24. Babichev, V.N.; Dem'yanov, A.V.; Dyatko, N.A.; Pal', A.F.; Starostin, A.N.; Filippov, A.V. Experimental and Theoretical Study of the Near IR Emission of Xenon Excited by a Fast Electron Beam. *Plasma Phys. Rep.* **2017**, *43*, 515–532. [CrossRef]
25. Smirnov, B.M. *Excited Atoms*; Energoizdat: Moscow, Russia, 1982; p. 232. (In Russian)
26. Lide, D.R. (Ed.) *CRC Handbook of Chemistry and Physics*, 84th ed.; CRC Press: Boca Raton, FL, USA, 2003.
27. Zaitsev, I.; Litvina, A.D.; Mogutnov, B.M.; Fridlyander, I.N.; Shelkova, N.E. An Investigation of Evaporation of Lithium. *High Temp.* **2001**, *39*, 507–510. [CrossRef]

Disclaimer/Publisher's Note: The statements, opinions and data contained in all publications are solely those of the individual author(s) and contributor(s) and not of MDPI and/or the editor(s). MDPI and/or the editor(s) disclaim responsibility for any injury to people or property resulting from any ideas, methods, instructions or products referred to in the content.